

# Volume illumination for two-dimensional particle image velocimetry

C D Meinhart<sup>†</sup>, S T Wereley<sup>‡</sup> and M H B Gray<sup>†</sup>

<sup>†</sup> Department of Mechanical & Environmental Engineering, University of California, Santa Barbara, CA 93106, USA

<sup>‡</sup> Department of Mechanical Engineering, 1288 Mechanical Engineering Building, Purdue University, West Lafayette, IN 47907, USA

Received 5 August 1999, in final form and accepted for publication 23 February 2000

**Abstract.** In particle image velocimetry experiments where optical access is limited or in microscale geometries, it may be desirable to illuminate the entire test section with a volume of light, as opposed to a two-dimensional sheet of light. With volume illumination, the depth of the measurement plane must be defined by the focusing characteristics of the recording optics. A theoretical expression for the depth of the two-dimensional measurement plane is derived and it is shown to agree well with experimental observations. Unfocused particle images, which lie outside the measurement plane, create background noise that decreases the signal-to-noise ratio of the particle-image fields. Results show that the particle concentration must be chosen judiciously in order to balance the desired spatial resolution and signal-to-noise ratio of the particle-image field.

**Keywords:** fluid flow velocity, particle image velocimetry, microfluidics, MEMS

## 1. Introduction

Since the 1980s, particle image velocimetry (PIV) has become a popular method for measuring spatially resolved velocity fields (Adrian 1986, Adrian and Yao 1985). The convention for two-dimensional PIV is to illuminate a single plane of the flow with a light sheet whose thickness is less than the depth of field of the image recording system. In this situation, the depth of the measurement plane is determined by the thickness of the light sheet.

Volume illumination is an alternative approach, whereby the test section is illuminated by a volume of light. This mode of illumination has been used to measure three-dimensional velocity vectors using a single camera (Willert and Gharib 1992), multiple cameras (Okamoto *et al* 1995) and a holographic camera (Gray and Greated 1993, Hinsch 1995).

Volume illumination may be necessary for obtaining two-dimensional measurements when optical access is limited to only one direction or in microscale geometries in which alignment of the light sheet is difficult. Volume illumination is advantageous when one is interested in measuring flows through micro electromechanical systems (MEMS) for which optical access is limited to one direction and the length scale is of the order of micrometres (Meinhart and Zhang 2000).

Usually, optical access inside silicon-based microfluidic devices is limited to one direction, because of the fabrication process. These devices can be fabricated by bulk

micromachining flow structures into a silicon substrate and sealed by anodically bonding borosilicate glass to the silicon structure. Devices constructed in this manner allow optical access from one direction only, through the glass wafer. In principle, waveguides can be micromachined directly into microfluidic devices (Sobek *et al* 1993, Foquet *et al* 1998) to provide optical access for a light sheet. Because of the added complexity involved during fabrication, using waveguides for optical access is not a desirable approach.

The small length scales associated with microfluidic devices require that the thickness of the measurement plane should be only a few micrometres. Since it is difficult to form a light sheet that is only a few micrometres thick and virtually impossible to align such a light sheet with the optical plane, volume illumination is the only feasible illumination method for most micro-PIV applications.

To date, microscale fluid measurements have consisted largely of bulk measurements, such as of volume flow rates, pressures and forces. A few researchers have made notable contributions towards making quantitative multi-point measurements of microflows. For instance, Brody and Yager (1996) calculated velocities based on microscopic particle streaklines. Paul *et al* (1998) used fluorescent microscopic imaging of a caged dye and scalar image velocimetry techniques to calculate velocities in a circular capillary. Lanzillo *et al* (1997) used x-rays scattered by emulsion droplets to image flow through optically opaque devices. These techniques suffer from having a large depth of field and hence the velocities measured are averaged through



where  $n$  is the refractive index of the fluid between the microfluidic device and the objective lens,  $\lambda_0$  is the wavelength of light in a vacuum being imaged by the optical system,  $NA$  is the numerical aperture of the objective lens,  $M$  is the total magnification of the system and  $e$  is the smallest distance that can be resolved by a detector located in the image plane of the microscope (for the case of a CCD sensor,  $e$  is the spacing between pixels). Equation (6) is the summation of the depth of field resulting from diffraction (the first term on the right-hand side) and geometrical effects (the second term on the right-hand side).

The cut-off for the depth of field due to diffraction (the first term on the right-hand side of equation (6)) is chosen by convention to be one quarter the out-of-plane distance between the first two minima in the three-dimensional point spread function, i.e.  $u = \pm\pi$  in figure 2. Substituting  $NA = n \sin \theta \simeq na/f$  and  $\lambda_0 = n\lambda$  yields the first term on the right-hand side of equation (6).

If a CCD sensor is used to record particle images, the geometrical term in equation (6) can be derived by projecting the CCD array into the flow field and then considering the out-of-plane distance the CCD sensor can be moved before the geometrical shadow of the point source occupies more than a single pixel. This derivation is valid for small light collection angles, for which  $\tan \theta \simeq \sin \theta = NA/n$ .

### 2.3. The PIV measurement depth

The measurement depth of volume-illuminated two-dimensional PIV can be defined as twice the distance from the centre of the object plane at which a particle can be located such that its maximum image intensity is an arbitrarily specified fraction of its maximum in-focus intensity. Beyond this distance, the particle-image intensity is sufficiently low that it will not significantly influence the velocity measurement. We will use  $\phi$  to denote this fractional intensity.

While the PIV measurement depth is related to the depth of field of the optical system, it is important to distinguish between these two concepts. The depth of field is defined as twice the distance from the object plane in which the object is considered unfocused in terms of image quality. In the case of volume-illuminated PIV, one is primarily interested in the measurement depth, which is defined as twice the distance from the object plane in which a particle becomes sufficiently unfocused that it no longer contributes significantly to the velocity measurement. In general, the depth of field and measurement depth are related quantities, but they are usually not equal.

The theoretical contribution of an out-of-focus particle to the correlation function is estimated by considering (i) the effect due to diffraction, (ii) the effect due to geometrical optics and (iii) the finite size of the particle. For the current discussion, we shall choose the cut-off for the on-axis image intensity,  $\phi$ , to be arbitrarily a tenth of the in-focus intensity. This arbitrary choice will be supported experimentally below.

The effect of diffraction can be evaluated by considering the intensity of the point spread function along the optical axis. From equation (5), if  $\phi = 0.1$ , then the intensity cut-off will occur at  $u \approx \pm 3\pi$ . Using equation (3), substituting

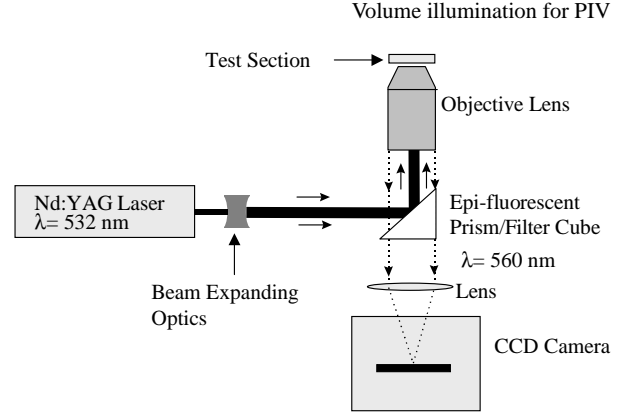


**Figure 3.** A schematic diagram of the micro-PIV system. Light ( $\lambda = 532$  nm) is emitted from the Nd:YAG laser and relayed through the objective lens into the test section, where it illuminates a volume of the test section. Fluorescently dyed particles in the test section are excited by the green  $\lambda = 532$  nm light and emit red  $\lambda = 570$  nm light. This light is imaged by the objective lens, passed through the epi-fluorescent filter cube and recorded by the CCD camera.

$\delta z_d = 2z$  and using the definition of numerical aperture,  $NA \equiv n \sin \theta \approx na/f$ , one can estimate the measurement depth due to diffraction as

$$\delta z_d = \frac{3n\lambda_0}{NA^2}. \quad (7)$$

The effect of geometrical optics upon the measurement depth can be estimated by considering the distance from the object plane in which the intensity along the optical axis of a particle with a diameter,  $d_p$ , decreases by an amount  $\phi = 0.1$ , due to the spread in the geometrical shadow, i.e. the collection cone of the lens. If the light flux within the geometrical shadow remains constant, the intensity along the optical axis will vary roughly as  $z^{-2}$ . From figure 1, if the geometrical particle image is sufficiently resolved by the CCD array, the measurement depth due to geometrical optics can be written for an arbitrary value of  $\phi$  as

$$\delta z_g = \frac{(1 - \sqrt{\phi})}{\sqrt{\phi}} \frac{d_p}{\tan \theta} \quad \text{for } d_p > \frac{e}{M}. \quad (8)$$

There may exist situations in which the pixel size (projected onto the object plane),  $e/M$ , is much larger than the particle diameter,  $d_p$ , and consequently equation (8) would not be applicable. In this case, the measurement depth is twice the distance at which the geometrical shadow is distributed over enough pixels that the intensity at any one pixel is reduced by an amount  $\phi$ . If the intensity distribution is uniform in the geometrical shadow (a good first approximation), one can show this depth to be

$$\delta z_g = \frac{(\frac{4}{\pi\phi})^{1/2} \frac{e}{M} - d_p}{\tan \theta} \quad \text{for } d_p \ll \frac{e}{M}. \quad (9)$$

Most PIV experiments are designed so that the particle images are sufficiently resolved by the CCD pixels. Therefore, we will only consider equation (8) in the current discussion. By setting  $\phi = 0.1$  and then adding the diameter of the particle to the measurement depth due to diffraction

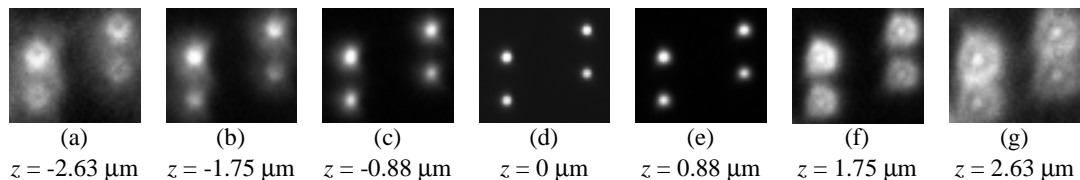


**Figure 4.** Particle-image fields of 1  $\mu\text{m}$  diameter polystyrene particles recorded using an  $M = 60$ ,  $NA = 1.4$  oil-immersion objective lens. Each of the images is taken at 1  $\mu\text{m}$  steps of the objective lens, corresponding to 0.88  $\mu\text{m}$  steps of the object plane. Image (d) is near the focal plane and is well focused. At approximately 1.75  $\mu\text{m}$  from the focal plane, images (b) and (f) are sufficiently unfocused that they do not contribute significantly to the correlation function. This corresponds to the maximum image intensity of a tenth of the maximum in-focus image intensity.

and geometrical optics, we obtain an estimate for the total measurement  $\delta z_m$ :

$$\delta z_m = \frac{3n\lambda_0}{NA^2} + \frac{2.16d_p}{\tan\theta} + d_p. \quad (10)$$

## 2.4. Experimental measurements

Experiments were performed to determine the accuracy with which equation (10) predicts the measurement depth, using the micro-PIV system shown in figure 3. In order to test the various terms in equation (10), we obtained a series of particle images with the objective lens at several discrete axial positions, using two different microscope objectives and particles of two different sizes. We used polystyrene particles of diameters  $d_p = 200$  nm and 1.0  $\mu\text{m}$ , which were fluorescently tagged to excite at  $\lambda_{abs} = 540$  nm and emit at  $\lambda_{emit} = 570$  nm. This fluorescent dye was chosen because its excitation frequency closely matched  $\lambda = 532$  nm light from the frequency-doubled Nd:YAG laser. The particle images were recorded using a  $1300 \times 1030$  pixel  $\times$  12-bit interline-transfer, cooled CCD camera. The interline-transfer feature of the camera allows one to acquire two back-to-back images within 500 ns. An air-immersion objective lens with a magnification  $M = 40$  and a numerical aperture  $NA = 0.6$  and an oil-immersion objective lens with  $M = 60$  and  $NA = 1.4$  were used to record the particle images.

A thin layer of a dilute particle solution was placed between a slide and a coverslip, so that particles would adhere to the coverslip surface. The microscope objective was positioned so that a group of particles deposited on the coverslip was in focus. A sequence of images was recorded as the microscope objective lens was translated axially in 1  $\mu\text{m}$  increments. When an oil-immersion objective lens was used to record particles immersed in a water solution, a 1  $\mu\text{m}$  displacement of the objective lens resulted to first order in a  $n_w/n_i = 1.33/1.515 = 0.88$   $\mu\text{m}$  displacement of the objective plane. Here,  $n_w/n_i$  is the ratio of the indices of refraction of the water solution and the lens immersion medium. Likewise, when an air-immersion lens was used to record images of particles immersed in a water solution, then a 1  $\mu\text{m}$  displacement of the objective lens resulted in a  $n_w/n_i = 1.33/1.0 = 1.35$   $\mu\text{m}$  displacement of the objective plane.

A sequence of particle images is shown in figure 4. The particles are 1  $\mu\text{m}$  diameter polystyrene and the images are recorded with an oil-immersion  $M = 60$ ,  $NA = 1.4$  objective lens. The image shown in figure 4(d) is well focused

**Table 1.** A comparison of measured depths of correlation calculated from experiments and theory.

$NA$	$M$	$n$	$d_p$ ( $\mu\text{m}$ )	$\delta z_m$ ( $\mu\text{m}$ )	
				Experiment	Theory (equation (10))
1.4	60	1.515	0.2	1.75	1.8
1.4	60	1.515	1.0	3.5	3.4
0.6	40	1.0	1.0	10.6	8.6

and near the object plane. At approximately 1.75  $\mu\text{m}$  from the focal plane, images (b) and (f) are sufficiently unfocused that they do not contribute significantly to the correlation function. The average maximum image intensity of images (b) and (f) is approximately a tenth of the maximum in-focus image intensity, which corresponds to the cut-off value chosen in the derivation of equation (10).

The measurement depth was estimated quantitatively by averaging the maximum intensity of six particles in each image. The average maximum intensity of each image was then plotted as a function of the axial position. The measurement depth was determined as twice the axial distance from the object plane where the intensity was reduced to a tenth of the maximum in-focus intensity. Table 1 compares the measurement depths obtained experimentally with theoretical values predicted by equation (10).

The experimentally determined measurement depths range from approximately  $\delta z_m = 1.8$   $\mu\text{m}$ , for an  $M = 60$ ,  $NA = 1.4$  objective lens imaging  $d_p = 200$  nm particles, to approximately  $\delta z_m = 10.6$   $\mu\text{m}$ , for an  $M = 40$ ,  $NA = 0.6$  objective lens imaging  $d_p = 1$   $\mu\text{m}$  particles. These results are in good agreement with the theoretical predictions of equation (10).

Since water has an index of refraction of  $n_w = 1.33$ , the effective  $NA$  of the oil-immersion lens when one is imaging into water can be estimated by multiplying the specified  $NA$  by the ratio  $n_w/n_i = 1.33/1.515 = 0.878$ . Therefore, the effective numerical aperture of the oil-immersion lens when one is imaging into water is  $NA_{eff} \approx 1.23$ .

It is important to note that the human eye accommodates from about 22 cm to infinity, therefore the measurement depth cannot be determined by peering directly into the microscope (Inoué and Spring, 1997). When viewing particles directly with the human eye, the particles appear to stay in focus over a larger range of axial distances than would particles that are imaged onto a CCD camera.

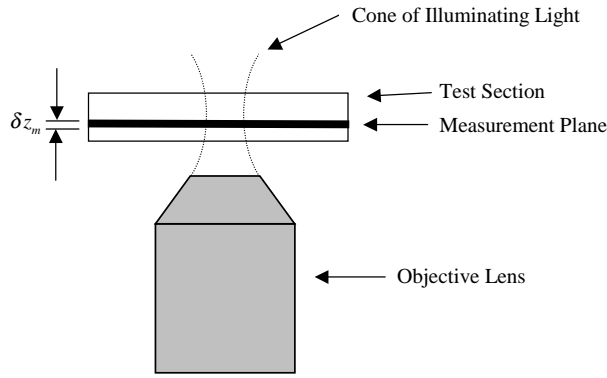


**Figure 5.** The geometry of the objective lens and test section. In the epi-fluorescence mode, light emanating from the objective lens illuminates a volume of the test section, which is defined by the cone of illumination. All the particles in the cone of illumination emit light, but only those particles within the measurement plane are sufficiently focused that they contribute to the correlation function.

### 3. Background noise

In volume-illuminated two-dimensional PIV, all particles within the cone of illumination (irrespective of whether they are in focus or out of focus) are illuminated and therefore emit light that contributes to the recorded image field, see figure 5. Particles that are outside the measurement domain (i.e. out of focus) increase the background noise level, which reduces the signal-to-noise ratio of the image field. For the current discussion, we define the signal-to-noise ratio of the image field to be the peak image intensity of a typical in-focus particle divided by the average background intensity. The signal-to-noise ratio depends upon many parameters: the particle size, particle concentration, test-section geometry, illumination, recording optics, CCD camera, etc.

For a fixed illumination depth (i.e. test-section thickness), the level of background noise can be lowered by decreasing the concentration of seed particles. A lower concentration of seed particles may require one to use larger interrogation regions to obtain an adequate correlation signal, which reduces the spatial resolution of the measurements. Likewise, higher spatial resolutions can be obtained in thinner test sections, because higher particle concentrations (and consequently smaller interrogation spots) can be used while maintaining an adequate signal-to-noise ratio.

The measured signal-to-noise ratio was estimated from particle-image fields taken of four different particle concentrations and four different device depths. The particle solution was prepared by diluting  $d_p = 200$  nm diameter polystyrene particles in de-ionized water. Test sections were formed using two feeler gauges of known thicknesses, sandwiched between a glass microscope slide and a coverslip. The particle images were recorded near one of the feeler gauges to minimize errors associated with variations in the test-section thickness, which could result from surface tension or deflection of the coverslip. The images were recorded with an oil-immersion  $M = 60$ ,  $NA = 1.4$ , objective lens.

The signal-to-noise ratios for four test-section depths and four particle concentrations are shown in table 2.

**Table 2.** Signal-to-noise ratios of the in-focus particle-image field for various particle concentrations and test-section depths.

Test-section depth ( $\mu\text{m}$ )	Particle concentration (by volume)			
	0.01%	0.02%	0.04%	0.08%
25	2.2	2.1	2.0	1.9
50	1.9	1.7	1.4	1.2
125	1.5	1.4	1.2	1.1
170	1.3	1.2	1.1	1.0

As expected, the results indicate that, for a given particle concentration, a higher signal-to-noise ratio is obtained by imaging through a thinner device. This result occurs because decreasing the thickness of the test section decreases the number of out-of-focus particles, while the number of in-focus particles remains constant. In general, thinner test sections allow higher particle concentrations to be used, which can be analysed using smaller interrogation regions. Consequently, the seed particle concentration must be chosen judiciously so that the desired spatial resolution can be obtained, while maintaining adequate image quality (i.e. signal-to-noise ratio).

### 4. Conclusions

The measurement depth of two-dimensional volume-illuminated PIV is related to the depth of focus of the recording lens and is dependent upon diffraction, geometrical optics and the particle size. Experimental measurements agree closely with theoretical predictions, which vary between 1.75 and 10.6  $\mu\text{m}$  for microscope objectives with numerical apertures of  $NA = 1.4$  and 0.6 and particle sizes of 0.2 and 1.0  $\mu\text{m}$ , respectively.

Background noise, resulting from out-of-focus particles that are volume illuminated, decreases the signal-to-noise ratio in the particle-image field. The signal-to-noise ratio can be improved by increasing the ratio of in-focus particles to that of out-of-focus particles. This can be accomplished by (i) increasing the measurement depth, (ii) decreasing the depth of the test section and (iii) decreasing the particle concentration.

### Acknowledgments

This work is supported by the AFOSR/DARPA (grant F49620-97-1-0515), DARPA (grant F33615-98-1-2853) and NSF (grant CTS-9874839).

### References

- Adrian R J 1986 An image shifting technique to resolve directional ambiguity in double-pulsed velocimetry *Appl. Opt.* **25** 3855–8
- Adrian R J and Yao C S 1985 Pulsed laser technique application to liquid and gaseous flows and the scattering power of seed materials *Appl. Opt.* **24** 44–52
- Born M and Wolf E 1997 *Principles of Optics* (Oxford: Pergamon)
- Brody J and Yager P 1996 Low Reynolds number microfluidic devices *Technical Digest. Solid State Sensors and Actuator Workshop (3–6 June 1996, Hilton Head, SC)* 105–8

- Foquet M, Han J, Lopez A, Wright W and Craighead H 1998 Fabrication of microcapillaries and waveguides for single molecule detection *Proc. SPIE* **3258** 141–7
- Gray C and Greated C A 1993 A processing system for the analysis of particle displacement holograms *Proc. SPIE* **2005** 636–47
- Hinsch K D 1995 Three-dimensional particle velocimetry *Meas. Sci. Technol.* **6** 742–53
- Inoué S and Spring K 1997 *Video Microscopy: The Fundamentals* (New York: Plenum)
- Lanzillotto A-M, Leu T-S, Amabile M, Santaney R and Wildes R 1997 A study of the structure and motion of fluidic microsystems *28th AIAA Fluid Dynamics Conf. Snowmass Village, CO*
- Meinhart C D, Wereley S T and Santiago J G 1999a PIV measurements of a microchannel flow *Exp. Fluids* **27** 414–9
- 1999b Micron-resolution velocimetry techniques *Developments in Laser Techniques and Applications to Fluid Mechanics* ed R J Adrian *et al* (Berlin: Springer)
- Meinhart C D and Zhang H-S 2000 The flow structure inside a microfabricated inkjet printhead *J. MEMS* **9** 67
- Okamoto K, Hassan Y A and Schmidl W D 1995 Simple calibration technique using image cross-correlation for three dimensional PIV *Flow Visualization and Image Processing of Multiphase Systems* ed W J Yang *et al* (New York: ASME) pp 99–106
- Paul P H, Garguilo M G and Rakestraw D J 1998 Imaging of pressure- and electrokinetically driven flows through open capillaries *Anal. Chem.* **70** 2459–67
- Santiago J G, Wereley S T, Meinhart C D, Beebe D J and Adrian R J 1998 A particle image velocimetry system for microfluidics *Exp. Fluids* **25** 316–19
- Sobek D, Young A M, Gray M L and Senturia S D 1993 A microfabricated flow chamber for optical measurements in fluids *Proc. IEEE Micro Electro Mechanical Systems Workshop, (Fort Lauderdale, FL)* pp 219–24
- Willert C E and Gharib M 1992 Three-dimensional particle imaging with a single camera *Exp. Fluids* **12** 353–8